

# Analysis of Multidimensional and Two-Phase Flows in Solid Rocket Motors

Sergei S. Bondarchuk,\* Aleksander B. Vorozhtsov,† Evgenii A. Kozlov,‡ and Yurii V. Feshchenko\*  
*Research Institute of Applied Mathematics and Mechanics, Tomsk 634050, Russia*

A physicomathematical model describing the processes in the combustion chamber of solid rocket motors (SRMs) is suggested. The model can be used in practical calculations of the parameters of real motors with solid-propellant charges of complex geometry. The model allows the description of two-phase flows (from averaged zero dimensional to three dimensional) for the complete operation cycle of SRMs, including transition to steady-state operating conditions and pressure drop accompanying the propellant burnout. Equations obtained can readily be employed in designing computer codes. Methods for the solution of these equations are discussed. Results of studying the gasdynamics parameters of internal flows are reported. Calculated values are compared with experimental data obtained for a modeled gas flow turning from the head-end to the charge channel. A three-dimensional calculation of flow parameters in a slotted-tube charge of a large-size motor is illustrated by distribution patterns for pressure and velocity. The influence of the redistribution of aluminum in a solid-propellant charge on the combustion efficiency coefficient of the metal, specific impulse, and in-chamber losses is analyzed.

## Nomenclature

$A$	= gas-permeable surface
$a$	= mass concentration
$B$	= pre-exponential factor
$C_p$	= specific heat of gas components or mixture
$c_i$	= specific heat of particles of the $i$ th fraction
$D$	= whole surface of grains forming igniter
$d$	= particle diameter
$E_c$	= ratio of propellant activation energy to universal gas constant
$e$	= web thickness of igniter grain
$f$	= friction stress
$G$	= mass supply from burning pyrotechnic composition
$H$	= width of channel
$H_0$	= enthalpy of flow products
$h(d)$	= function of mass distribution of particles in size
$I$	= Vilyunov's parameter
$K$	= number of fractions of condensed phase
$L$	= number of gaseous components of mixture
$M$	= mass supply density
$n$	= unit vector of external normal to surface
$p$	= pressure
$Q$	= ratio of propellant explosion heat to propellant specific heat
$q$	= heat flux density
$r$	= burning rate
$S$	= gas-impermeable surface
$T_c$	= condensed-phase temperature
$T_g$	= temperature of gaseous combustion products
$T_i$	= particle temperature
$u$	= velocity vector
$V$	= volume
$W$	= interior free volume
$x$	= axial coordinate
$y$	= axis normal to propellant surface
$z$	= portion of condensed phase in combustion products

$\gamma$	= adiabatic index (ratio of specific heats)
$\epsilon$	= erosion coefficient
$\kappa$	= thermal diffusivity of solid propellant
$\lambda_c$	= frictional drag coefficient for plate
$\rho$	= density
$\rho_0$	= igniter density
$\rho_i$	= mass concentration of particles of $i$ th fraction
$\varphi$	= combustion efficiency of metal
$\omega_i$	= volume of grains

## Introduction

WIDESPREAD use of solid rocket motors (SRMs), particularly in space vehicles, including manned ones,<sup>1</sup> attaches special significance to works concerned with developing and improving methods for calculating motor operation conditions. At the moment, the investigation, design, and development of SRM all involve mathematical simulation.<sup>2–6</sup> The processes in SRM combustion chambers responsible for thrust and specific impulse depend on propellant burning rate that is determined by physicochemical characteristics of the propellant and by local flow parameters in the vicinity of the burning surface. Therefore, calculation of the gas flowfield at the burning surface is an urgent problem.

At present, the design of advanced propulsion systems and propellant charge geometry has significantly departed from traditional patterns. The charges of SRM are characterized by the complexity of propellant formulations that include considerable amounts of metal additives and by the complex geometry of the burning surface. The multiphase flows (including burning metal particles) of combustion products require multidimensional description. Among the current challenges of simulation and computation of in-chamber processes are the development of universal techniques for the solution of sophisticated problems, in particular, those involving two- and three-dimensional description of flows. In many cases, the gasdynamics parameters must be calculated in terms of a multidimensional nonstationary problem,<sup>5</sup> taking into account the multiphase nature of the flow.<sup>7,8</sup> However, since these methods are time- and labor-consuming, it is reasonable to apply them only to problems where a detailed flow pattern is required. Information needed for the estimation of integral characteristics can be obtained in terms of a one-dimensional approach or by averaging the parameters over the volume of the combustion chamber.

Received Sept. 24, 1994; revision received Jan. 30, 1995; accepted for publication Feb. 6, 1995. Copyright © 1995 by the American Institute of Aeronautics and Astronautics, Inc. All rights reserved.

\*Ph.D., Senior Researcher.

†Professor, Head of Department.

‡Professor, Deputy Director.

Calculation of the gasdynamics of in-chamber processes must take into account the main physicochemical phenomena taking place during motor operation. For example, the combustion of metallized solid propellant in SRM involves such specific kinds of losses as two-phase loss and loss by incomplete burning of metal.<sup>8</sup> In some cases, on the other hand, a particular goal of the calculation is to disregard certain factors. To be adequate, the calculations should be based on multilevel computation programs involving multidimensional description of the problem (from volume-averaged to three dimensional) and must take into account the variety of physical processes.

In this work we suggest a physicomathematical model, and report results of the solution of practical problems arising during the design and development of SRM.

### Mathematical Formulation of the Problem

It is assumed that the mixture of the gaseous combustion products of solid propellant and igniter, the gasification products of thermal insulation materials, and the initial gas obey the equation of state for an ideal nonviscous gas. The dissipation effects caused by friction and heat exchange of gas with bounding surfaces and with condensed particles in the gas flow are taken into account through additional source terms. The system of equations is applied to a reference volume  $V$  bounded by a closed surface comprised of gas-permeable  $A$  and gas-impermeable  $S$  materials, where heat and mass exchange between gas flow and SRM elements occur. The system of equations for the principal laws of conservation is written in the integral form in generalized coordinate systems.

conservation of mass

$$\frac{\partial}{\partial t} \int_V \rho \, dV + \int_A \rho N \, dA = \int_S \sum_{j=1}^L (1 - z_j) M_j \, dS$$

$$N = (\mathbf{u} \cdot \mathbf{n}) \quad (1)$$

conservation of momentum

$$\frac{\partial}{\partial t} \int_V \rho \mathbf{u} \, dV + \int_A (\rho \mathbf{n} + \rho \mathbf{u} N) \, dA + \int_S (\rho \mathbf{n} + \rho \mathbf{u} N) \, dS$$

$$+ \int_S \rho \mathbf{f} \, dS + \int_V \sum_{i=1}^K \rho_i \mathbf{f}_i \, dV = 0, \quad N = (\mathbf{u} \cdot \mathbf{n}) \quad (2)$$

conservation of energy

$$\frac{\partial}{\partial t} \int_V E \, dV + \int_A (E + p) N \, dA + \int_V \sum_{i=1}^K \rho_i (\mathbf{u} \cdot \mathbf{f}_i + q_i) \, dV$$

$$+ \int_S q \, dS = \int_S \sum_{j=1}^L H_{0j} (1 - z_j) M_j \, dS \quad (3)$$

total energy

$$E = p/(\gamma - 1) + \rho |\mathbf{u}|^2/2 \quad (4)$$

Real in-chamber flows experience various chemical transformations that add complexity to the mathematical description of the process. In terms of the ideal-gas model, the chemical reactions can be taken into account approximately if their rates are treated as infinite or zero (equilibrium and frozen flows, respectively). Because the assumption of equilibrium flows requires rather cumbersome and time-consuming computations, there is little sense in using this approach in practical calculations for motors of real geometry unless the calculation is treated as an end in itself.

Methodologically, the assumption of a frozen flow is more simple to realize. Therefore, it is more widely used in solving

the problems of interior ballistics of SRM. This assumption implies no chemical reactions, with thermodynamic properties of the mixture-gas "constant"  $R$ , specific heat  $C_p$  at constant pressure, and specific heat ratio being determined through the concentrations of mixture components  $a_j$  by the equations:

$$R = \sum_{j=1}^L a_j R_j, \quad C_p = \sum_{j=1}^L a_j C_{pj}$$

$$\gamma = \frac{C_p}{C_p - R}, \quad \sum_{j=1}^L a_j = 1 \quad (5)$$

The system of Eqs. (1–4) is complemented with the equations of law of mass conservation for the components. This is required for calculation of local thermodynamic properties

$$\frac{\partial}{\partial t} \int_V \rho a_j \, dV + \int_A \rho a_j N \, dA = \int_S (1 - z_j) M_j \, dS$$

$$j = 1, 2, \dots, L \quad (6)$$

The efficiency of the approach and, in particular, of its computation programs can be improved by multiplying Eq. (6) for each component by the gas constant and adding the result for the entire mixture:

$$\sum_{j=1}^L R_j \frac{\partial}{\partial t} \int_V \rho a_j \, dV + \sum_{j=1}^L R_j \int_A \rho a_j N \, dA$$

$$= \sum_{j=1}^L R_j \int_S (1 - z_j) M_j \, dS \quad (7)$$

Comparison of this equation with Eq. (5) and similar transformations for  $C_p$  yield the final relationships:

$$\frac{\partial}{\partial t} \int_V \rho R \, dV + \int_A \rho R N \, dA = \int_S \sum_{j=1}^L R_j (1 - z_j) M_j \, dS \quad (8a)$$

$$\frac{\partial}{\partial t} \int_V \rho C_p \, dV + \int_A \rho C_p N \, dA = \int_S \sum_{j=1}^L C_{pj} (1 - z_j) M_j \, dS \quad (8b)$$

Thus, the component concentration Eqs. (6) are replaced by Eqs. (8a) and (8b) for the local thermodynamic characteristics of the mixture  $C_p$  and  $R$ . Since the number of components in the problems under discussion is, as a rule, more than two (the combustion gasification products of igniter and of multicomponent solid propellant, the products of thermal insulation, initial gas, etc.), the advantages of the described approach are apparent. Usually up to five equations for a six-component mixture are considered. It is important that the right sides of Eqs. (8) take into account variations in  $R$  and  $C_p$  in the course of the process, e.g., depending on combustion conditions. This fact is rather essential in calculations since the gas constant and specific heat of combustion products for some propellant compositions (particularly igniter compositions) vary widely with pressure rise from initial to operational, which cannot be taken into account by traditional treatments set by Eq. (6). The local value of gas temperature is calculated according to the ideal gas law

$$T_g = p/(\rho R) \quad (9)$$

The mass burning rate of a propellant as a function of flow parameters is determined as corrected for the initial temperature of charge, unsteadiness, and the effect of erosion. The correction factor for the burning rate as a function of the initial temperature of the composition is given by one of the experimental linear fractional, exponential, or power dependencies. The correction for the burning rate unsteadiness

is calculated by the phenomenological model of Zeldovich–Novozhilov,<sup>9</sup> which assumes a slow response of the condensed phase. In terms of this model, the burning rate is determined by the instantaneous pressure over the burning surface and by the temperature gradient at the burning surface which, in turn, is derived from the problem of nonstationary thermal conductivity formulated for the condensed phase. The erosion coefficient, equal to the ratio of the burning rates and taking into account the effect of the blowing gas flow, is presented as a function of the dimensionless parameter  $I$  proposed by Vilyunov<sup>10</sup>:

$$\varepsilon = 1 + \varepsilon_*(I - I_*), \quad I = (\rho u / \rho_0 r) \sqrt{\lambda_c} \quad (10)$$

where the asterisks mark the experimental values of reference parameters.

The description of the interaction of the flow of hot gases in a SRM chamber with members of the construction is attained by means of experimental criterial dependencies and is determined by the geometry of the calculation domain, flow regime, and dimensionality of the problem. The software developed for the approach proposed in this article offers the user a number of universally known experimental and theoretical dependencies (the laws of Reynolds, Blasius, Prandtl, Schlichting, and Nikuradze, etc.), as well as the dependencies obtained specifically for SRM and even for particular motors, propellants, igniters, etc. For certain laws describing the friction and heat exchange coefficients at the surfaces that bound the flow of combustion products, corrections are introduced (from a list suggested to user) for the nonadiabatic behavior of the flow, the compressibility of the medium, and the efflux from the surface, based on the relative correspondence method.<sup>11</sup>

The effective emissivity factor of the system's gas surface, needed for calculation of the radiation component of the heat flux, is determined through the superposition of the approximate solutions of the equations for the radiation transfer in the cases of "pure" gas and an extremely particle-laden (for SRM) flow of combustion products, depending on the diameter and volume concentration of particles, the pressure and temperature of the carrier medium, and the optical thickness of the flow region.

The system of equations describing the condensed phase motion is formulated on the following assumptions. We assume that the particles flowing together with the combustion products of solid propellant and igniters form a polydisperse system of  $K$  fractions; the function  $h(d)$  of the mass distribution of particles in size is considered to be a given. The nonisothermic flow of the heterogeneous mixture in the channel is treated as the motion of two interacting and interpenetrating media.<sup>12,13</sup> The coagulation and fragmentation of particles are disregarded and the influence of the disperse phase on gas density is ignored. Taking into account the above mentioned assumptions, the principal laws of conservation of mass, momentum, and energy for the condensed phase have the form

$$\frac{\partial}{\partial t} \int_V \rho_i dV + \int_A \rho_i N_i dA = \int_S \sum_{j=1}^L z_j M_j h_j dS \quad (11)$$

$$\frac{\partial}{\partial t} \int_V \rho_i u_i dV + \int_A \rho_i u_i N_i dA = \int_V \rho_i f_i dV$$

$$\begin{aligned} \frac{\partial}{\partial t} \int_V E_i dV + \int_A E_i N_i dA &= \int_V \rho_i (u_i f_i + q_i) dV \\ &+ \int_S \sum_{j=1}^L z_j M_j T_{s_j} h_j c_j dS \end{aligned} \quad (12)$$

$$E_i = \rho_i (c_i T_i + |u_i|^2/2), \quad N = (u_i, n), \quad i = 1, 2, \dots, K \quad (13)$$

The dynamic and thermal interphase interaction is described by equations relating the experimental criterial dependencies of friction and heat exchange coefficients to the parameters of the gasdynamic and condensed-phase flows.<sup>7,12</sup>

One of the difficult problems to be solved in parallel with obtaining the gasdynamic flowfield is that of calculating the ignition of a solid–propellant surface element during the transition of SRM to steady-state operation. The ignition time is calculated in terms of the condensed-phase ignition theory developed by Vilyunov<sup>14</sup> and other authors. It is assumed that the ignition of the surface element occurs instantaneously with the surface temperature rise up to a critical value, at which point the heat flux generated in the propellant surface layer becomes larger than the incident heat flux.<sup>5,14</sup> The mathematical problem in the ignition of a condensed substance (solid propellant) involves the equation of thermal conductivity taking into account the heat release term and the equation of chemical kinetics<sup>15</sup>:

$$\begin{aligned} \frac{\partial T_c}{\partial t} &= \kappa \frac{d^2 T_c}{dy^2} + QF(a, T_c) \\ \frac{\partial a}{\partial t} &= -F(a, T_c) \end{aligned} \quad (14)$$

The rate  $F(a, T_c)$  of the chemical reaction is set by the Arrhenius dependence  $F(a, T_c) = Ba \cdot \exp(-E_c/T_c)/\rho_0$ .

The effect of hot gaseous combustion products on the charge is simulated by establishing the boundary conditions of the third kind at the solid–propellant surface and by setting the heat flux at infinity to be zero.

Simulation of the transition of motor operation to steady-state regime involves consideration of a number of processes, the least understood of which being those related to igniter action and heat exchange between the hot combustion products of igniting compositions and solid propellant. The gases flowing from the igniter to the combustion chamber warm up and ignite successively the parts of the propellant surface. The thermal effect of the gases finally determines the behavior of the pressure–time curve during transition of the motor to steady-state operation. The parameters of heat exchange between the igniter combustion products and solid propellant, apart from other factors, depend essentially on the operation mode of the igniter.

The problems involved in calculating igniter performance have received considerable attention.<sup>2,4,5</sup> Two main types of igniters were considered: igniters with consumable casings and those with indestructible casings. In the first case, when the igniter casing is destroyed in the course of operation, it is reasonable to use the well-proved approach that implies that the igniter grains are ignited simultaneously and their mass distribution along the SRM channel is described by an exponentially decreasing function; the mass and energy supply due to igniter combustion is incorporated in the source terms of gasdynamics equations.

Igniters of the second type (indestructible casing, e.g., a perforated cylinder), characterized by more stable performance, have received wide acceptance in real SRM. In this case, the mathematical model describing the variation of gasdynamic parameters in the volume of the igniter casing is a system of usual differential equations for interior-ballistics characteristics averaged over the interior free volume  $W$  (lumping or zero-dimensional description). It is assumed that the entire surface of  $D$  grains forming the igniter is ignited instantaneously, and that the perforated casing prevents the escape of grains. The system of equations of the principal laws of conservation of mass and energy and of variation in the free interior volume of the igniter then becomes

$$\frac{d}{dt}(\rho W) = \sum_{i=1}^D (1 - z_i) G_i - M_* \quad (15a)$$

$$\frac{d}{dt}(\rho RW) = \sum_{i=1}^D (1 - z_i) R_i G_i - RM_* \quad (15b)$$

$$\frac{d}{dt}(\rho C_p W) = \sum_{i=1}^D (1 - z_i) C_{pi} G_i - C_p M_* \quad (15c)$$

$$\frac{d}{dt} \left( \frac{pW}{\gamma - 1} \right) = \sum_{i=1}^D (1 - z_i) C_{pi} T_{pi} G_i - \frac{1}{\gamma - 1} \frac{p}{\rho} M_* \quad (15d)$$

$$\frac{dW}{dt} = - \sum_{i=1}^D \frac{d\omega_i}{dt} \quad (15e)$$

The mass supply  $M_*$  through the perforation holes is calculated by the familiar equations of the quasistationary theory.<sup>4,5</sup> The mass supply rate of gas  $G_i$  is related to the change in the volume of burning igniter material as follows:

$$G_i = -\rho_{oi} \frac{d\omega_i}{dt}, \quad i = (1, 2, \dots, D) \quad (16)$$

There is a simple relationship between the current volume of grains  $\omega_i$  and their characteristic sizes. The change in the characteristic grain size during combustion is described as

$$\frac{de_i}{dt} = -r_i, \quad i = (1, 2, \dots, D) \quad (17)$$

The gasdynamic flowfield was calculated by the finite volume method,<sup>16</sup> where the flows through volume boundaries were determined from solution of the Riemann problem<sup>17</sup> or by the method of large particles.<sup>18</sup>

A computer code developed by the authors calculates the field of gasdynamic parameters in several different ways: for one- two- and three-dimensional geometry as well as for the geometry of "intermediate" dimensionality, when one calculation well is used for one (or two) direction(s) and all three velocity vector components are considered. It is also possible to calculate the subregions in terms of different dimensionalities, including averaging the gasdynamic parameters over the subregion volume. Traditional methods for calculating the heating and ignition of a solid propellant are based on solution of a parabolic equation of thermal conductivity with the Arrhenius source term for a semi-infinite layer of propellant. Since the temperature rise conditions and rate are not given, a sufficiently accurate preliminary estimation of the depth of the preheated layer is impossible. Thus, it is unreasonable (from the viewpoint of the accuracy of calculating the zone of maximum gradients) to use the finite difference scheme with a constant integration step. In the approach suggested, therefore, Eqs. (14) are solved using an adaptable calculation grid that is varied depending on the warming-up condition.<sup>15</sup> The main idea of the adaptation is to use explicit operators of transition to another time layer for a difference grid whose nodes move at a linearly increasing velocity from zero at the propellant surface to a certain maximum value in the last node. The velocity of the last node depends on the velocity of the isotherm of a fixed temperature that is 5–10 K higher than the initial temperature. The expression for the velocity is derived from the relationship of the finite difference scheme operator setting the transition to the next time layer. Use of the explicit scheme to solve the heat conduction equation in this case sets no additional limits on time step since the step of integration with respect to time is limited by the value employed for the solution of Eqs. (1–4). A detailed description and analysis of the approximation, stability, and convergence of the proposed method for solution of the thermal conductivity equation as applied to calculation of the ignition of the solid propellant surface has been described elsewhere.<sup>15</sup>

The above theoretical background and use of appropriate initial and boundary conditions allow the calculation of SRM

performance during the entire operation period. Transition to steady-state operation is realized on the basis of nonstationary equations under initial conditions characteristic of the initial state of the motor. The quasistationary operation of SRM is simulated by the same equations in terms of the stabilization method, wherein the steady-state solution is treated as the limiting case of the transient case. Here, the initial distribution of flow parameters is set either by the final results of the transition to operation regime, or approximately by the gasdynamic functions.<sup>2,4,5</sup> Such an approach is reasonable since the stabilization method allows arbitrary initial conditions, and the convergence of the solution is determined in the main by specific and appropriate realization of boundary conditions. The final period of pressure decay in an SRM is treated by nonstationary gasdynamic equations under the initial conditions characteristic of the end of quasi-steady-state operation of the motor. In solving the previously mentioned problems, when deemed necessary, blocks are used to model the change in motor geometry due to charge and casing strains and propellant burning, and to describe the destruction of thermal insulation materials. Each block is a separate complex problem and is not considered in this article.

The mathematical model is realized in program blocks that allow parallel calculations.

## Calculation Results

### Two-Dimensional Flows

Calculation results for a two-dimensional flow were compared with experimental data obtained on a setup modeling a gas flow at the head-end cavity and in the channel of an SRM. Cold gas was injected into the channel (see Fig. 1) from its upper bounding surfaces (33 m/s from the inlet cavity and 1.5 m/s from the channel surface of width  $H$ ). The gas flowed out through the right open end of the channel.

Figure 1 shows the field of the velocity vector of the gas flow. The flow pattern suggests, as might be expected, that the velocity vector varies in both direction and magnitude mostly in the region of flow turn (the junction of the inlet cavity and the channel). A sufficiently uniform velocity profile in the vicinity of the inlet orifice is gradually deformed; the maximum distortion of the profile is observed in the vicinity of the cavity-channel junction. Figure 2 shows the lines representing the constant pressure related to the external pressure. A stagnation zone (region of high pressure, 7.1 kPa, and low velocity) is formed at the bottom of the front wall of the inlet cavity. A similar zone is formed behind the shelf formed by the bottom of the inlet cavity and the front wall of the channel below its inlet orifice. The gas pressure and flow velocity at the upper wall of the channel above the shelf

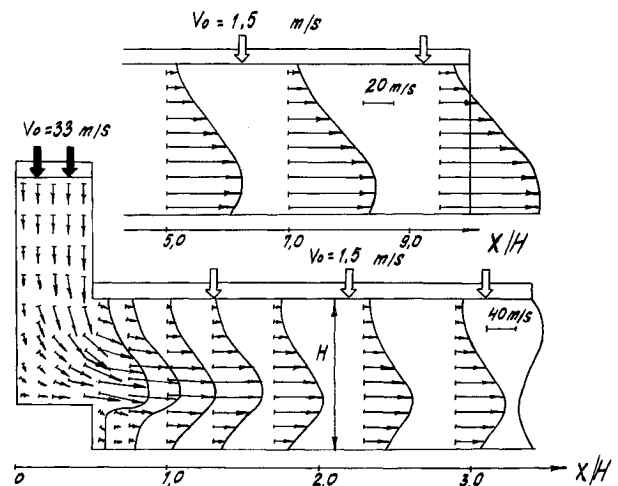


Fig. 1 Calculated velocity field in a simulated experimental setup.

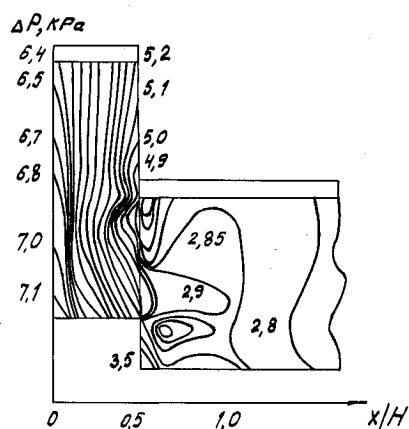


Fig. 2 Calculated pressure field in a simulated experimental setup.

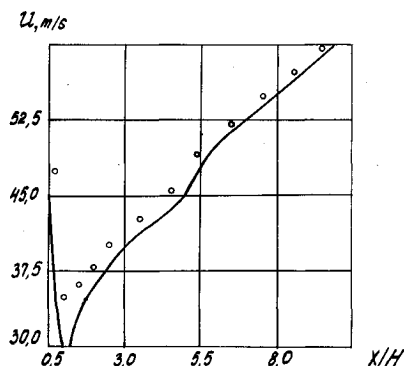


Fig. 3 Calculated and experimental values of flow velocity at lower bounding surface (calculation;  $\circ$ , experiment).

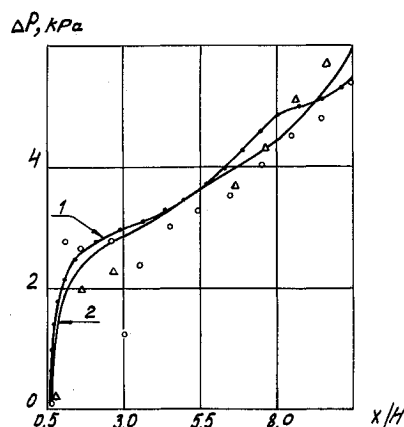


Fig. 4 Calculated and experimental values of total and static pressure difference related to pressure at channel inlet; total pressure (1, calculation;  $\circ$ , experiment), static pressure (2, calculation;  $\Delta$ , experiment).

are considerably lower (Fig. 2). In the inlet section of the channel, up to  $x/H \approx 3$ , the velocity inlet up to  $x/H \approx 5$ . Less coincidence is observed between the experimental and calculated dependencies of the total and static pressure difference (Fig. 4) related to the pressure at the channel inlet. Solid lines represent calculated data, curve 1 and circles denote total pressure, curve 2 and triangles indicate static pressure. The maximum difference in the results is observed (as in the previous case) in the inlet section of the channel in the zone of flow stabilization. In general, however, experimental and calculated results show good agreement.

### Three-Dimensional Flows

Three-dimensional flow was simulated for a large SRM with a slotted-tube charge during motor transition to steady-state

operation. Isobars in Fig. 5 show the pressure distribution in the combustion chamber. The pressure magnitudes are related to a reference value determined from mass and energy balances in the SRM chamber under critical conditions of isentropic flow of gases through the nozzle.<sup>4</sup> Figure 4 shows that as the nozzle inlet recessed into the combustion chamber is approached, the relatively equal distances between isobars are reduced and their profile is distorted due to a complex interaction of counterflows. A high-pressure region is formed in the zone of the encountering flows. Then, as the motor aft end is approached, the distances between the isobars increase near the nozzle; the pressure difference approaches zero in the stagnation zone at the aft end within the SRM casing. The same figure shows the velocity distribution corresponding to the pressure distribution in the zone of the recessed nozzle. As the inlet of the recessed nozzle is approached, the profile (practically uniform in the channel and uniformly inclined in the slot) is deformed, particularly in the regions in which the gas efflux from the slot to the channel. Figure 6 shows the distribution of the transverse velocity of gas in the cross section A-A. The flow pattern (velocity vector field) that occurs during filling of the stagnation zone in the vicinity of the aft closure due to pressure rise in the combustion chamber is shown in Fig. 7. Solid lines indicate the disposition of slot axes in the charge. This flow pattern is determined by the more intense compression of gas flow in those regions near the slots.

A number of other problems of practical gasdynamics have been solved; one-dimensional, quasi-two-dimensional and, quasi-three-dimensional versions of the method have been checked. The problems concerned with high-temperature gas

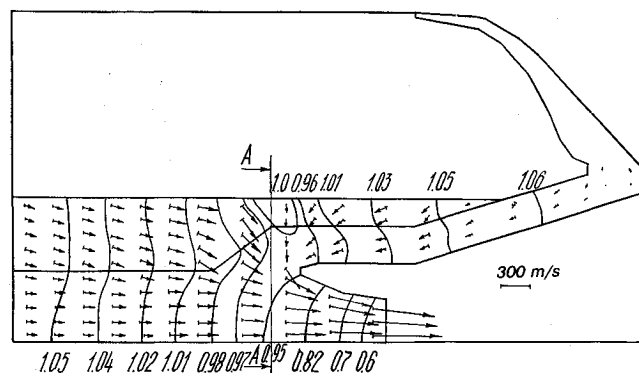


Fig. 5 Distribution of velocity and pressure vectors in combustion chamber of a large-size motor.

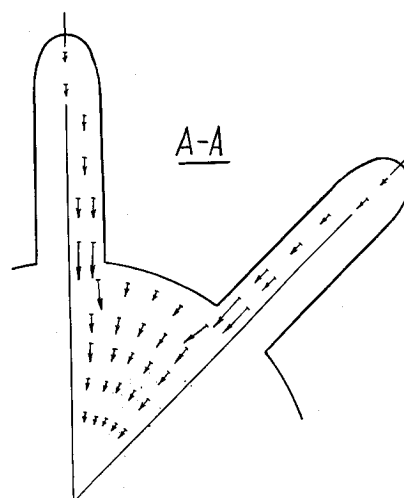


Fig. 6 Velocity distribution in cross section of slotted-tube charge.

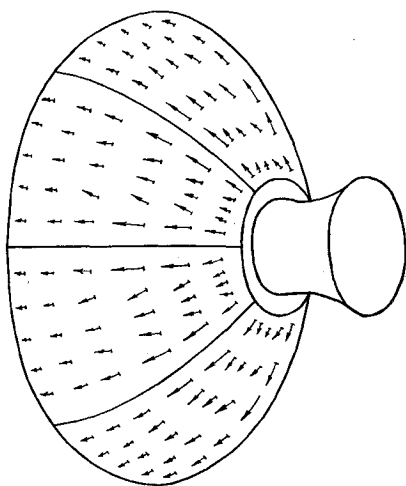


Fig. 7 Flow over end (nozzle) closure.

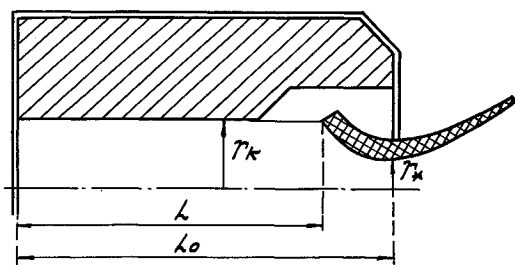


Fig. 8 Calculated region.

flows in pipelines of complex geometry were studied and the dynamics of flow structure in combustion chambers with movable nozzles as well as other problems were analyzed. Calculations have confirmed the high reliability and efficiency of the proposed approach. The calculation results are in good agreement with available experimental data.

#### Two-Phase Flows

In the investigation of two-phase flows containing burning aluminum particles, equations for gaseous oxidizer and metal concentrations were added along with an equation for single particle burning.<sup>7,8</sup> The parameters of a two-phase polydisperse flow were investigated by test calculations of the gas-dynamics in a semiconfined channel (Fig. 8) with a radius-to-length ratio  $r_k/L_0 = 0.1$ . The mass burning rate decreased linearly along the channel from 25 kg/m<sup>2</sup>s at  $x = 0$  to 20 kg/m<sup>2</sup>s at  $x = L$ . The concentration of the oxidizing agents was 50%, the percentage of Al/Al<sub>2</sub>O<sub>3</sub> being 22 weight %. Five size fractions of particles with the following mass fractions were used: 20  $\mu$ , 60%; 50  $\mu$ , 10%; 100  $\mu$ , 10%; 150  $\mu$ , 10%; and 200  $\mu$ , 10%. It was assumed that the particles of all fractions contained 25% pure metal. Figure 9 shows the velocity distributions for gas (curve 0) and particles of the 1–4 fractions (curves 1–4) over the channel length. The increasing gas velocity gradient increases the difference in the velocity of gas and particles of each fraction along the channel; the larger the particles, the greater the difference. Figure 10 presents the correlation between particle size and temperature in a two-phase flow. The change in the combustion efficiency of aluminum contained in the particles of the two-phase flow is shown in Fig. 11. The completeness of Al combustion is determined for the nozzle throat location for particles entering the flow in different locations along the charge length. Analysis of the calculation results makes it possible to determine the boundary from which the particles of the particular fraction (curves 1–5) entering the flow make their contribution to the net decrease in the combustion efficiency of aluminum.

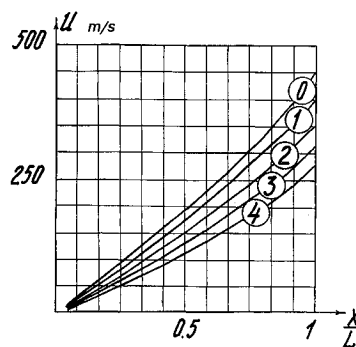


Fig. 9 Distribution of gas (curve 0) and particle (curves 1–4) velocities along channel.

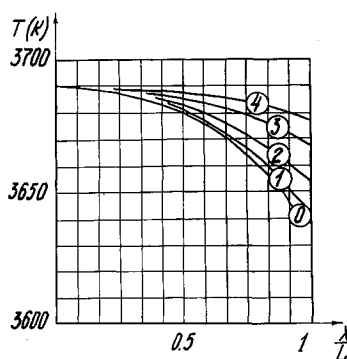


Fig. 10 Distribution of gas (curve 0) and particle (curves 1–4) temperatures along channel.

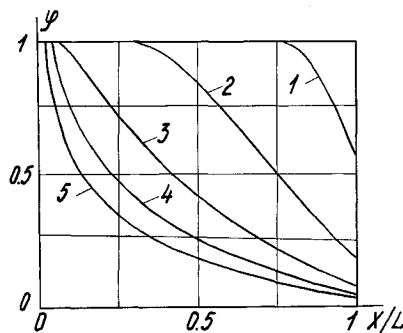


Fig. 11 Variation in combustion efficiency of metal in particles of 1–5 fractions (curves 1–5, respectively), along channel.

The in-chamber loss in specific impulse due to inefficient combustion of metal can be reduced by optimizing the distribution of the metallized additive in solid propellant charge in order to increase its combustion efficiency. The residence time of metal particles and agglomerates in the combustion chamber should be longer than the time for metal burnout. A natural method of decreasing the loss of specific impulse is to redistribute the metal in the bulk of the charge so that residence time of particles in the chamber extends and combustion efficiency increases, with the average aluminum content of composite solid propellant corresponding to the maximum value of theoretical specific pressure impulse.

For qualitative consideration of the effect of the condensed phase on the combustion efficiency of metal, an SRM with a case-bonded charge was investigated. The SRM parameters were: nozzle throat radius  $r_* = 0.15$  m, channel radius  $r_k = 0.26$  m, charge length to recessed section of nozzle  $L = 1.38$  m, and total length of channel  $L_0 = 1.61$  m. The pressure in the head end of the chamber was  $p(x = 0) = 6.5$  MPa.

The aluminum content of the propellant was 22.7%. It is well-known that the size distribution function of the agglom-

**Table 1** Mass size distribution of the agglomerates of Al

$d, \mu$	$h$	$d, \mu$	$h$
20	0.0025	75	0.1550
30	0.0400	90	0.1200
40	0.1100	120	0.0600
50	0.2500	150	0.0400
65	0.2025	200	0.0200

erates entering the flow from the surface of solid propellant is characterized by two modes. Assuming that the particles of the first mode (microns) are burnt out and consist of aluminum oxide, we consider only the influence of the particles of the second mode (50  $\mu$ , 10%; 75  $\mu$ , 40%; 100  $\mu$ , 30%; 150  $\mu$ , 10%; 200  $\mu$ , 10%) on the combustion efficiency of the metal. The percentage of second-mode particles is such that the coarse-grained fractions contain 7% of the initial amount of aluminum.

The previous assumptions were used in the following set of calculations:

1) Al is uniformly distributed over the channel length (traditional version). The calculated combustion efficiency of aluminum is  $\varphi = 88.1\%$ .

2) Al is redistributed uniformly in the head section of the charge, with 0.08 charge length from the aft end containing no metal. The calculated combustion efficiency is  $\varphi = 89.2\%$ .

3) Al is redistributed uniformly in the head section of the charge, with 0.16 charge length from the aft end containing no metal. The calculated combustion efficiency is  $\varphi = 90.3\%$ .

4) Al content in the charge varies linearly from 32.7% in the head section to 12.7% in the aft section. The calculated combustion efficiency is  $\varphi = 97.1\%$ .

Thus, it is seen that the combustion efficiency is higher when the metal is redistributed to the head section of the charge. Consider now the calculation results for a polydisperse two-phase flow with burning metal particles in the charge channel of a large SRM with the following parameters:  $L = 2.75$  m,  $r_k = 0.48$  m,  $r_* = 0.18$  m,  $p(x = 0) = 7.5$  MPa, and  $T_g = 3690$  K. An experimental histogram of the size distribution of the agglomerates (the data were obtained by O. G. Glotov in the laboratory of V. E. Zarko, Institute of Chemical Kinetics and Combustion, Novosibirsk), coming to the flow of combustion products is given in Table 1.

The content of pure aluminum in fractions with particles less than 20  $\mu$ m is below 0.5%, the other fractions contain 17–23% pure metal. Given the traditional  $d_{43}$  at the nozzle inlet, the two-phase loss is 3.0 s. The calculated values of specific pressured impulse and metal combustion efficiency coefficient are 165.6 s and 95.4%, respectively.

At an Al distribution in the charge where a constant total percentage of the metal is absent in the one-sixth charge length at the aft section, the calculation yields the following values: specific impulse 167 s and metal combustion efficiency 100%.

Note that the gain obtained by redistributing metal in the charge is rather considerable.

### Conclusions

The results of this work present a real possibility for controlling the combustion efficiency of metallized propellants by means of metal redistribution. The investigations pointed out the necessity of an improved physicomathematical model

of a two-phase flow in the combustion chamber of an SRM which could describe the (entire) evolution of metal particles, including agglomeration, coagulation, and fragmentation from the burning surface to the nozzle inlet. In the present work, we restricted ourselves to the search for possible lines of inquiry. The authors realize that this is a problem of optimization, and its solution must provide the functional dependencies of metal distribution in the charge on the determining parameters of the problem. In addition, formulation of the problem should take into account variations in physicochemical and physicomechanical parameters of charge caused by redistribution of metal, changes in mass-geometry characteristics during motor operation in a real rocket, etc. Of interest also is analysis of metal redistribution, not only in length but also in the bulk of the charge, with due account taken of the characteristic features of particular constructions.

### References

- <sup>1</sup>Zakharov, A. G., and Nazarov, Yu. K., "Transport Space System," *Itogi Nauki i Tekhniki, ser. Raketostroenie*, Vol. 7, VINITI, Moscow, 1976.
- <sup>2</sup>Erokhin, B. T., and Lipanov, A. M., *Unsteady-State and Quasi-Steady-State Operation of Solid-Propellant Rocket Motors*, Mashinostroenie, Moscow, 1977.
- <sup>3</sup>Alemasov, V. E., Dregalin, A. F., and Tishin, A. P., *Theory of Rocket Motors*, Mashinostroenie, Moscow, 1977.
- <sup>4</sup>Sorkin, R. E., *Theory of In-Chamber Processes in Solid-Propellant Rocket Motors*, Nauka, Moscow, 1983.
- <sup>5</sup>Raizberg, B. A., Erokhin, B. T., and Samsonov, K. P., *Fundamentals of the Theory of Operation Processes in Solid-Propellant Rocket Motors*, Mashinostroenie, Moscow, 1972.
- <sup>6</sup>Kozlov, E. A., Vorozhtsov, A. B., and Bondarchuk, S. S., "Practical Gas Dynamics of In-Chamber Processes in Solid-Propellant Rocket Motors," *Fizika*, Vol. 35, No. 8, 1992, pp. 104–114.
- <sup>7</sup>Vilyunov, V. N., Vorozhtsov, A. B., and Feshchenko, Yu. V., "Modeling of Two-Phase Flow of a Mixture of Gas and Burning Metal Particles in a Semi-Confined Channel," *Fizika Gorenia i Vzryva*, Vol. 25, No. 3, 1989, pp. 39–43.
- <sup>8</sup>Vilyunov, V. N., Vorozhtsov, A. B., and Feshchenko, Yu. V., "Evolution of a Polydisperse Ensemble of Burning Metal Particles in a Semi-Confined Channel," *Fizika Gorenia i Vzryva*, Vol. 28, No. 6, 1992, pp. 32–37.
- <sup>9</sup>Novozhilov, B. V., *Transient Combustion of Solid Propellants*, Nauka, Moscow, 1984.
- <sup>10</sup>Vilyunov, V. N., "On the Theory of Erosive Combustion of Powders," *Doklady Akademii Nauk SSSR*, Vol. 136, No. 2, 1960, pp. 381–384.
- <sup>11</sup>Motulevich, V. P., "Relative Correspondence Method and its Application to Heat and Mass Transfer Problems," *Inzhenerno-Fizicheskii Zhurnal*, Vol. 14, No. 1, 1968, pp. 7–16.
- <sup>12</sup>Vasenin, I. M., and Arkhipov, V. A., *Gas Dynamics of Two-Phase Flows in Nozzles*, Tomsk State Univ. Press, Tomsk, Russia, 1986.
- <sup>13</sup>Nigmatulin, R. I., *Foundations of Mechanics of Heterogeneous Media*, Nauka, Moscow, 1978.
- <sup>14</sup>Vilyunov, V. N., *Theory of Ignition of Condensed Substances*, Nauka, Moscow, 1984.
- <sup>15</sup>Borovskoy, I. G., Bondarchuk, S. S., Kozlov, E. A., and Vilyunov, V. N., "Solution of the Problem of Condensed System Ignition Based on a Difference Scheme with a Time-Dependent Grid," *Fizika Gorenia i Vzryva*, Vol. 22, No. 3, 1986, pp. 14–19.
- <sup>16</sup>Roache, P. J., *Computational Fluid Dynamics*, Hermosa Publishers, Albuquerque, NM, 1976.
- <sup>17</sup>Godunov, S. K. (ed.), *Numerical Solution of Multidimensional Problems of Gas Dynamics*, Nauka, Moscow, 1976.
- <sup>18</sup>Belotserkovsky, O. M., and Davydov, Yu. M., *Method of Large Particles in Gas Dynamics*, Nauka, Moscow, 1982.